
Filtration of kaolinite particles in a saturated porous medium: hydrodynamic effects

Abdellah Alem · Abdulghadir Elkawafi ·
Nasre-Dine Ahfir · HuaQing Wang

Abstract A study was undertaken on physical clogging of a porous medium by injecting suspended particles (SP), ranging in diameter from 1.7 to 40 μm , into a sand-filled column. Long-term tracer tests were carried out at various flow velocities. Retention of the SP is significantly influenced by the flow velocity. At low flow velocities, retention is confined to a limited length of porous medium, from the entrance of the column, leading to a substantial modification of the hydraulic characteristics of the porous medium. However, at high flow velocities, a much greater length of the porous medium is affected. Particle-size analyses indicate that the particle-size distribution (PSD) of recovered particles changes with time, while the PSD of retained particles changes with depth and time. At the beginning of the filtration process, larger particles were mainly retained at the column entrance. As the injection volume increases, the larger particles penetrate more deeply into the porous medium, and the size of particles observed in the effluent gradually increases. This study highlights the influence of flow velocity, duration of filtration, and the particles' polydispersity, on the hydraulic characteristics of the porous medium.

Keywords Hydraulic properties · Laboratory experiments · Polydispersity · Suspended particles · Clogging

Introduction

Clogging of porous media is an important process in both natural and engineered systems. It has been the subject of an intense research effort since the 1960s (Kehat et al. 1967; Herzig et al. 1970). The decrease of permeability

caused by particle deposition has been a concern for many industries such as the petroleum industry (Ochi and Vernoux 1999; Moghadasi et al. 2004), drinking water supply (Detay 1993) or artificial recharge of aquifers (Bouwer 2002; Vigneswaran and Suazo Ronillo 1987).

The phenomena involved in porous-media clogging are diverse and complex. Three mechanisms can be identified: (1) physical clogging, restricting particle movement in soil and other porous media (straining and filtration; McGechan and Lewis 2002); (2) biological clogging, caused by biological growth and the accumulation of by-products from the decomposition of biological growth (Hand et al. 2008; Brovelli et al. 2009); and (3) chemical clogging, that depends on chemical factors which control the colloidal stability of the particles and minerals precipitated from water (Compere et al. 2001; Mays and Hunt 2007).

The filtration performance of a porous medium is influenced by several factors: hydraulic conductivity of the medium (Reddi et al. 2005); particle concentration in the influent (Lee and Koplík 2001; Moghadasi et al. 2004); grain-size distribution (Lee and Koplík 2001; Moghadasi et al. 2004); pore-size distribution; and the geometry and surface-roughness of the grains (Tong and Johnson 2006; Shellenberger and Logan 2002). Previous studies indicate that the average overall retention of particles in a porous medium is not sufficient to predict clogging. These studies reveal that deposit morphology has an important influence on the degree of clogging (Boller and Kavanaugh 1995; Veerapaneni and Wiesner 1997; Mays and Hunt 2005, 2007).

Subsequent studies have revealed that the retention of particles is mainly influenced by physicochemical interaction (Khilar and Fogler 1984; Sen and Khilar 2006), hydrodynamics (Veerapaneni and Wiesner 1997; Ahfir et al. 2007, 2009), and physical straining (Bradford et al. 2002, 2003, 2006; Xu and Saiers 2009). Torkzaban et al. (2007) indicated that hydrodynamic and Derjaguin-Landau-Verwey-Overbeek (DLVO) forces and collector shape and size significantly influenced the colloid collision efficiency. Colloid attachment was only possible on regions of the collector where the torque from hydrodynamic shear acting on colloids adjacent to collector surfaces was less than the adhesive (DLVO) torque that resists detachment. The applied hydrodynamic torque will

Received: 14 February 2012 / Accepted: 3 December 2012
Published online: 8 January 2013

© Springer-Verlag Berlin Heidelberg 2013

A. Alem · A. Elkawafi · N.-D. Ahfir (✉) · H. Wang
Laboratoire Ondes et Milieux Complexes (LOMC),
UMR 6294 CNRS – Université du Havre,
53 Rue de Prony, BP 540, 76058 Le Havre cedex, France
e-mail: nasre-dine.ahfir@univ-lehavre.fr

increase with the water velocity, the particle size, and decreasing grain size. Under unfavourable attachment conditions, hydrodynamic forces can induce rolling of particles on the solid surface or promote release (Johnson et al. 2007).

For relatively large particles, straining, which represents the trapping of fine particles in down-gradient pore-throats that are too small to allow particle passage, could play an important and sometimes dominant role in their immobilisation in the porous medium. Recent findings indicate that the rate of particle straining within saturated porous media is sensitive to the ratio of particle diameter (d_p) to porous-medium grain diameter (d_g). Bradford et al. (2003) reported that straining contributes significantly to particle retention when the ratio d_g/d_p is greater than around 0.005. Experiments conducted with monodisperse and bidisperse particle suspensions suggested that colloid size-nonuniformity can have a significant impact on straining kinetics. Straining of larger particles was reduced by smaller particles, primarily due to faster depletion of straining capacity, while straining of smaller particles was enhanced by the presence of larger particles, due to blockage of pore openings by the larger particles (Xu and Saiers 2009).

The most common experimental technique for studying clogging phenomena is step-input injection of a suspension of particles in a column packed with porous materials. The injection is performed in a porous medium under constant hydraulic head or constant flow rate (Reddi et al. 2005). Many theoretical models have been devoted to describing depth-filtration processes. Phenomenological models, as developed by Herzog et al. (1970), also called macroscopic models, are based on resolution of mass-balance equations. These models use phenomenological laws of filtration and pressure evolution that are in accordance with macroscopic observations done during the experiments.

The aim of this paper is to investigate the physical-clogging process for a sandy porous medium in a controlled laboratory environment. Natural polydisperse suspended particles (kaolinite) were studied. The specific objectives of the study included: (1) examining the influence of flow velocity on the transport and deposition of kaolinite particles, which are polydisperse; and (2) understanding better how deposited particles affect the degree of clogging of the porous medium. To achieve these goals, special attention was given to transport and deposition of the particles under the conditions of long injection times. Effluent concentration curves, deposition profiles, temporal changes in the particle-size distribution of the effluent, and spatial and temporal changes in the deposited particle-size distribution, were measured. Based on these multiple observations, relevant mechanisms that control the transport and deposition of these polydisperse particles are discussed. In addition to these measurements, pressure variations along the porous medium during injection were measured, allowing damage to the porous medium to be evaluated in space and time. The effects of flow velocity and the retention mechanisms on damage to the porous medium are discussed.

Materials and methods

The step-input injection method is a technique for studying transport and filtration mechanisms of suspended particles (SP) in saturated porous media in the laboratory. In this investigation, a Plexiglas column with an inner diameter of 4.1 cm and a length of 40 cm was used. The column was equipped with eight piezometers, allowing pressure variations during the injection process to be measured. The column was packed in 5-cm increments by pouring the material (sand) into the column, mixed with deionised water (under saturated conditions) to avoid trapping air bubbles. The column was fed by reservoirs containing deionised water (pH of 6.9 ± 0.2) and the SP, using a Cole-Parmer Masterflex peristaltic pump. A digital McMillan flow-meter was installed at the column inlet to measure the flow rate (Fig. 1).

The porous medium that filled the column during the experiments consisted of sand collected from the Seine River (France), with grain-size selection being performed by sieving. The grain-size distribution of the sieved sand ranged from 315 to 630 μm , with a mean diameter of 410 μm . Scanning electron microscopy images showed that the sand grains were a mixture of angular and round in shape with very rough surfaces. The injected SP consisted of size-selected particles of Kaolinite P300. According to the particle-size distribution of the SP, acquired using a Coulter Multisizer II particle counter, the particle diameters ranged from 1.7 to 40 μm , with a modal diameter of 15 μm .

Before injecting the SP, permeability tests were carried out to characterize the porous medium (clean bed). The column was fed from the water tank under constant head. Measurements of different pressures along the length of the column allowed the overall permeability to be determined, along with the permeabilities of different sections of the porous medium (between two adjacent piezometers), thereby characterising the homogeneity of the porous medium. The permeability test was repeated for different magnitudes of constant head. The hydraulic conductivity was calculated using Darcy's law. The average hydraulic conductivity of the sand was $K = 7 \times 10^{-4} \text{ m/s}$. Using the bulk-density method, the porosity of the sand was found to be $\phi_0 = 0.37$.

The SP injection was done from the SP reservoir (Fig. 1). To prevent the deposition of particles on the interior surfaces of the reservoir, the particles were maintained in suspension with the help of a motorised stirrer. The detection system consists of a Kobold Instruments Turbidimeter, which has a measurement range of 1–5,000 NTU (nephelometric turbidity units). The particle concentrations in the effluent were determined with the help of correlations made a priori between measured SP concentrations in the water and values in NTU given by the detection system. The SP injection experiments were conducted with a constant injection concentration of $C_0 = 1 \text{ g/L}$. A total mass (M_{inj}) of 20 g of SP was injected in each experiment. The flow velocity was varied from 0.041 to 0.209 cm/s, simulating slow sand filtration and rapid sand filtration. Values for the Reynolds number for the

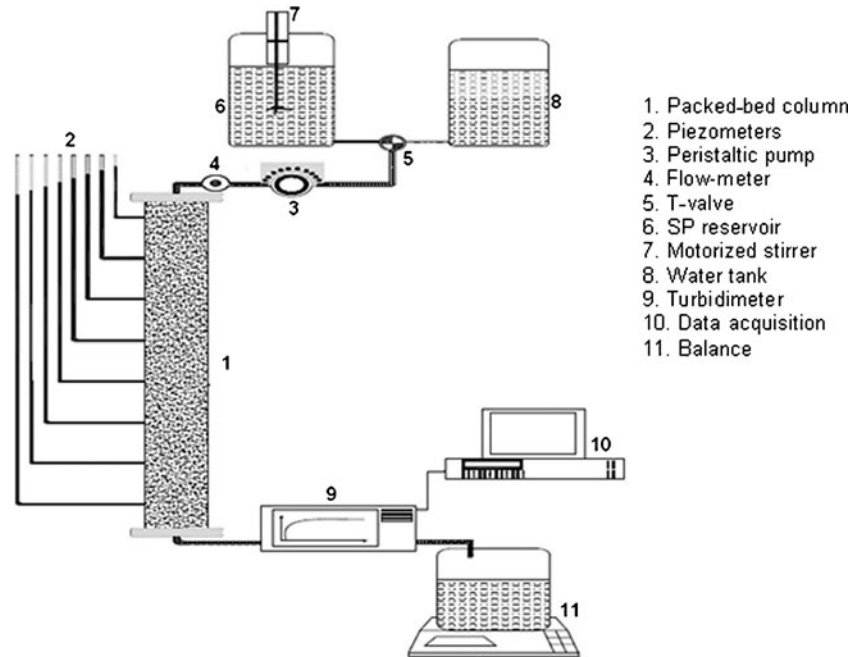


Fig. 1 Schematic diagram of the experimental set-up

porous medium, varying between 0.171 and 0.855, confirm that the experiments were conducted under laminar flow conditions (de Marsily 1986). Thus, Darcy’s law remains applicable in this investigation.

During the tracer experiments (injection tests), pressure variations in the porous medium along the length of the column were measured, together with SP concentrations at the outlet from the column. To determine the size of the particles transported out of the porous medium, samples were collected for microgranulometric spectral analysis with the Coulter Multisizer II particle counter.

At the end of each experiment, the material (sand with deposited SP) filling the column was divided into nine different sections (Fig. 2), in order to measure the amount of retained particles along the column. The weight of the deposited SP in each section was then determined, using the following procedure: the material from each section was dried and weighed, then thoroughly washed; the clean material (sand) was dried and weighed; the difference in weight between the dirty and clean materials gave the accumulated weight of deposited SP. Samples were collected from the wash water for microgranulometric spectral analysis with the Coulter Multisizer II particle counter.

A mass balance was conducted at the end of each column experiment using effluent concentration data and

the inal spatial distribution of retained particles in the porous medium. The calculated mass of particles in the effluent (M_{eff}) and those retained in the porous medium (M_p) were normalised by the total mass of particles injected into the column (M_{inj}), as shown in Table 1.

Modelling

The dynamics of particle deposition, in the transient stage, for a simple one-dimensional rectilinear case, can be described with a macroscopic mass conservation and rate equation, as follows (Herzig et al. 1970; Bai and Tien 2000):

$$\frac{\partial \sigma}{\partial \tau} + U \frac{\partial C_v}{\partial z} = 0 \tag{1}$$

$$\frac{\partial \sigma}{\partial \tau} = U \lambda C_v \tag{2}$$

where $\sigma [L^3.L^{-3}]$ is the retention defined as the volume of deposited particles per unit of porous-medium volume, $z [L]$ is the direction of suspension flow, $\tau [T]$ is the

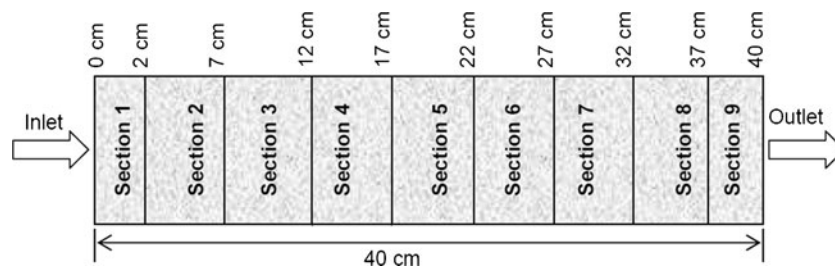


Fig. 2 Schematic representation of how the porous medium in the column was divided into nine different sections

corrected time defined as $\tau = t - z\phi/U$, with t [T] being the real time, ϕ [-] the porous-medium porosity and U [$L.T^{-1}$] the Darcy velocity. C_v [$L^3.L^{-3}$] is the volume fraction of particles in the suspension ($C_v = C/\rho_p$, where C [$M.L^{-3}$] is the mass fraction of particles in the suspension and ρ_p [$M.L^{-3}$] is the SP specific density). λ [L^{-1}] is the filter coefficient, which is considered constant only during the initial filtration period when the porous medium is still clean. In the transient stage, as deposition increases, a deterioration in particle removal is observed. Thus, λ varies with time and depth. λ can be related to retention σ , $\lambda = \lambda_0 F(\sigma)$, where λ_0 is the initial value of the filter coefficient (clean bed).

Based on experimental data, a number of empirical expressions for $F(\sigma)$ have been proposed by various authors. For a review on this subject, see for example Bai and Tien (2000) and Zamani and Maini (2009). For some expressions of $F(\sigma)$, analytical solutions exist (Herzig et al. 1970; Bai and Tien 2000; Zhang et al. 2000).

The initial conditions for a porous medium initially free of deposition are: $C_v(z,0)=0$, $\sigma(z,0)=0$, and the boundary condition is $C_v(0,t)=C_{v0}$.

If $F(\sigma)$ is described by the linear function of σ , $F(\sigma) = \left(1 - \frac{\sigma}{\sigma_{max}}\right)$, an analytical solution of Eqs. (1) and (2) is obtained and is given by (Bai and Tien 2000):

$$\frac{C_v(z, \tau)}{C_{v0}} = \frac{\exp\left(\frac{U\lambda_0 C_{v0} \tau}{\sigma_{max}}\right)}{\exp\left(\frac{U\lambda_0 C_{v0} \tau}{\sigma_{max}}\right) + \exp(\lambda_0 z) - 1} \quad (3)$$

and

$$\sigma(z, \tau) = \sigma_{max} \frac{\exp\left(\frac{U\lambda_0 C_{v0} \tau}{\sigma_{max}}\right) - 1}{\left(\exp\left(\frac{U\lambda_0 C_{v0} \tau}{\sigma_{max}}\right) + \exp(\lambda_0 z) - 1\right)} \quad (4)$$

where σ_{max} is the maximal retention.

For fitting the experimental breakthrough curves (BTCs) (for $z = L$, where L is the length of the porous medium), Eq. (3) can be rearranged into the following form:

$$\ln\left(\frac{C_v}{C_v(L, \tau)} - 1\right) = \ln(\exp(\lambda_0 L) - 1) - \left(\frac{U\lambda_0 C_{v0}}{\sigma_{max}}\right) \tau \quad (5)$$

From the intercept and gradient of the graph of $\ln\left(\frac{C_v}{C_v(L, \tau)} - 1\right)$ versus τ , the values of λ_0 and σ_{max} can be calculated. Once the values of λ_0 and σ_{max} are known, the profile of retention along the length of the porous medium at different times is then completely defined using Eq. (4).

Results and discussion

SP transport and retention in the porous medium

In this section, the influence of hydrodynamic effects is discussed. The BTCs (Fig. 3) are represented by a relative concentration (outlet concentration C_v divided by the constant inlet concentration C_{v0}) as function of the number of pore volumes injected (NVp). For all experiments, the BTCs show two very distinct filtration stages. The first is clean-bed filtration, called the clean-bed stage, which is only truly valid at the beginning of the filter process (Jegatheesan and Vigneswaram 2000). In this stage, particles already retained do not prevent the deposition of other particles in the suspension. After an injected volume about $2 NVp$ (two complete pore volumes), the BTCs reach a plateau (see the inset graph in Fig. 3) and remain constant until a critical NVp , which depends on the flow velocity. After that, the porous medium will start to accumulate particles and a deterioration in particle removal is observed, with the deposition leading to a gradual saturation of the retention sites. This stage of filtration is called the transient stage (Jegatheesan and Vigneswaram 2000). In this stage of filtration, the amount of particles already deposited in the porous medium influences the filtration of other particles (Jegatheesan and Vigneswaram 2000; Brown et al. 2002). Because of the limited number of retention sites in the porous medium accessible for the capture of particles, the SP removal decreases as these retention sites become occupied during filtration. Thus, the SP concentration in the effluent increases with time.

The BTCs depend strongly on the flow velocity. The flow velocity governs the hydrodynamic forces created in the pore space, which influence particle deposition. A high flow velocity results in higher hydrodynamic forces, which in turn reduce the likelihood of deposition. After injecting $83 NVp$, the relative concentration (C_v/C_{v0}) reached 83, 69 and 27 % for the Darcy velocities of 0.209, 0.125 and 0.041 cm/s, respectively. Notice that for the lowest flow velocity ($U=0.041$ cm/s), until $35 NVp$ had

Table 1 Mass balances: the SP mass percentages recovered in the column effluent (M_{eff}); deposited in each of the nine sections; in the porous medium overall (the sum of the nine sections) (M_p), and the total ($M_{tot} = M_{eff} + M_p$), for the different test velocities

Darcy velocity (cm/s)	Mass deposited in each section (%)									M_p (%)	M_{eff} (%)	M_{tot} (%)
	1	2	3	4	5	6	7	8	9			
0.041	10.96	19.36	18.11	12.81	12.14	9.04	7.46	4.70	2.14	96.73	5.41	102.14
0.083	11.12	17.89	13.86	10.46	6.90	5.92	5.44	4.97	2.99	79.56	19.77	99.33
0.125	6.75	9.87	8.30	6.66	4.95	4.75	3.96	3.30	2.50	51.03	48.90	99.93
0.167	6.48	10.16	6.58	5.44	4.06	3.79	3.48	3.48	1.91	45.33	57.96	103.29
0.209	5.91	9.79	5.77	4.35	3.75	3.46	3.39	2.56	2.02	40.97	61.60	102.57

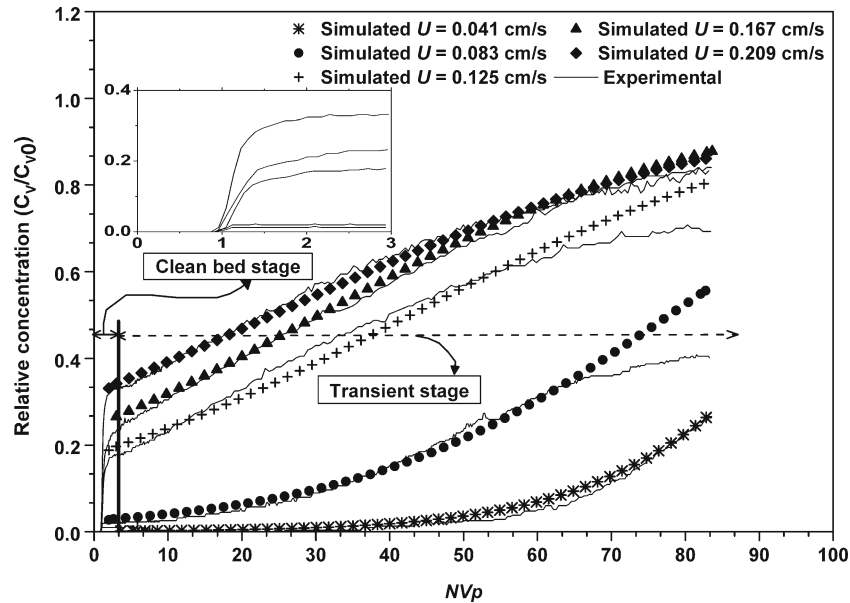


Fig. 3 Observed breakthrough curves of the SP (solid lines), plotted with simulated BTCs (symbols) for different Darcy velocities; BTCs for the clean-bed stage ($NVp \leq 3$) are shown in greater detail in the inset graph (parameters as defined in the text)

been injected, the hydrodynamic forces were too low to prevent SP deposition and are insufficient to allow the detachment and transport of previously deposited particles. Beyond 35 Vp injected, owing to the accumulation of SP deposited in pore spaces, local pressures increased sufficiently to cause the release of some of the previously deposited particles (Fig. 3).

The model predictions for BTCs are also shown in Fig. 3. The comparison shows good agreement between the modelling results and the experimental data for practically the whole period of the experiments, suggesting that the model provides a satisfactory prediction of global particle removal in the porous medium.

On Fig. 4, the initial filter coefficient (λ_0) and the maximal retention (σ_{\max}) as a function of the Darcy velocity (U) are plotted. The results show that λ_0 and σ_{\max} decrease when the flow velocity increases, and can be described by the following power relationship:

$$Y = a.U^{-n} \quad (6)$$

where “ a ” is a constant and “ n ” is the power coefficient, equal to 1.03 and 0.75 for λ_0 and σ_{\max} evolution, respectively. These coefficients are close to that reported by Wegelin (1996), who gave power coefficients equal to 0.88 and 0.8 for λ_0 and σ_{\max} evolution, respectively.

Spatial distribution of deposition

In order to obtain the deposition profile of the retained particles along the length of the porous medium at the end of the SP injection, the porous medium filling the column was cut into nine sections (Fig. 2). The mass of SP deposited in each section was determined using the measurement technique described in the Materials and methods section. Table 1 summarizes the SP mass

percentages recovered in the effluent (M_{eff}), deposited in each of the nine sections and in the porous medium overall (M_p), and the total ($M_{\text{tot}} = M_{\text{eff}} + M_p$) for the different tested velocities. Values of M_{tot} were somewhat different from M_{inj} , with the ratio $M_{\text{tot}}/M_{\text{inj}}$ ranging from 99 to 103 %. The difference between M_{tot} and M_{inj} can be attributed to measurement errors.

For each section of porous medium, an average retention was calculated, given as the ratio of the volume of deposited particles to the volume of the section. Figure 5a shows the retention profiles of the SP (denoted by σ) along the length of the porous medium (axial distance, on the horizontal axis), for different flow velocities at the end of each injection. The evolution of the retention profile during injection is depicted in Fig. 5b. The profiles in Fig. 5b were obtained by performing five tests with an identical flow velocity of 0.083 cm/s, and stopping the test at different times, corresponding to injected volumes equal to 10, 20, 30, 40 and 83 Vp , respectively. The results show that the retention is non-uniformly distributed in the porous space. The retention is very important at the entrance to the porous medium, but decreases with depth. Deeper parts of the porous medium contribute less to the removal of the SP and only at very advanced stages of filtration. The non-uniform distribution increases when the flow velocity decreases, favouring SP removal early in the filter. At a given depth, retention decreases with increasing flow velocity (Fig. 5a).

The experimental data and model prediction (Eq. 4) for retained particles along the porous medium are shown in Fig. 6. A significant deviation between model predictions of the distribution of deposited particles throughout the porous medium and the experimental data was observed, especially near the column entrance. Notice that the longer the experimental period is, the larger the deviation is between the model predictions and the experimental data

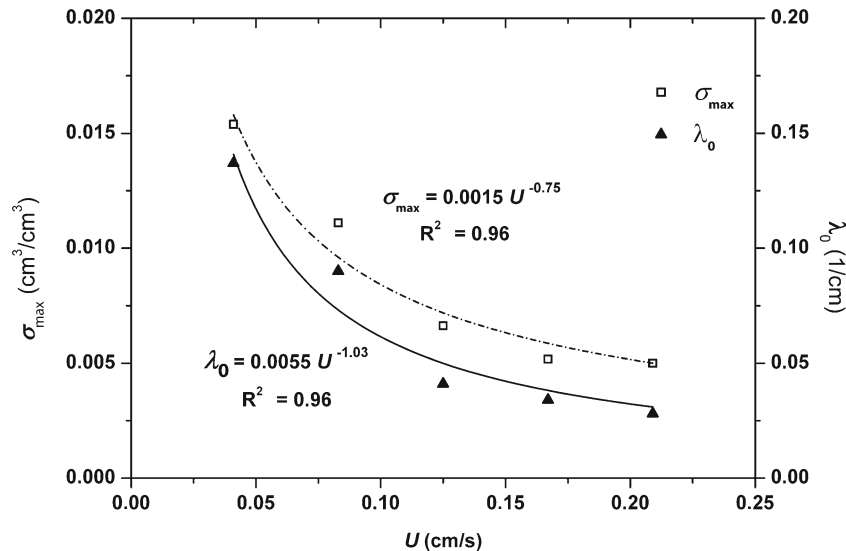


Fig. 4 Initial filtration coefficient λ_0 and maximal retention σ_{\max} as a function of flow velocity

(after 60 V_p). This suggests that straining plays an important role in filtration, mainly near the column entrance, as highlighted in the present study, with the same effect also being noticed by Bradford et al. (2002).

In the present study, the ratio (d_p/d_g) of the suspended particle size d_p (which ranged from 1.7 to 40 μm), to the mean grain size d_g (which was 410 μm), varied between 0.0041 and 0.0975. For SP with size greater than 2 μm (representing 98 % of the total mass of the injected SP), this ratio is greater than a critical value of 0.005, as recently reported in the literature (Bradford et al. 2003). This suggests that mechanical straining is a significant mechanism for the capture of SP in the filtration experiments, especially for larger particles ($d_p > 15 \mu\text{m}$). Also, as discussed in the preceding, even when the flow velocity is high, the retention near the inlet remains substantial (Fig. 5a) and then rapidly decreases with increasing distance from the inlet. This special distribution is consistent with straining behaviour, as reported by Bradford et al. (2002, 2003). As will be discussed in the section entitled *Particle-size analysis of the recovered and deposited SP*, straining is the main mechanism responsible for the retention of larger particles near the inlet to the porous medium.

The straining effect is not adequately described by the classical filtration model. A model with a filtration coefficient that depends on depth and on the ratio of particle diameter to median grain size would be more appropriate for the interpretation of the observed spatial distribution of retained particles.

Damage to the porous medium

The damage to the porous medium over time as a result of particle deposition was assessed by observing declines in either the permeability or porosity of the porous medium. As shown earlier (Fig. 5a), the flow velocity has a direct influence on the retention profile and consequently on the spatial and temporal evolution of the hydrodynamic

characteristics of the porous medium (Roque et al. 1995). Indeed, damage to the porous medium is not only a function of the volume of deposited SP, but also a function of the retention profile. Porosity is a parameter, directly related to permeability, which changes because of particle retention. That is why variation in porosity is also a factor in assessing the damage to a porous medium. In this investigation, the porosity (ϕ) at a given depth (z) is related to the volume of deposited SP, and determined by the following equation (Zamani and Maini 2009):

$$\phi(z, t) = \phi_0 - \frac{\sigma(z, t)}{(1 - \phi_d)} \quad (7)$$

where ϕ_0 is the initial porosity of the clean bed, and ϕ_d is the deposit porosity which depends on the morphology of the deposits formed.

The deposit porosity is derived from the average density of deposited particles as follows (Boller and Kavanaugh 1995):

$$\phi_d = 1 - \frac{\rho_d}{\rho_p} = 1 - \left[\frac{\rho_w}{\rho_p} + \left(1 - \frac{\rho_w}{\rho_p} \right) \frac{1}{a} N^{1-b} \right] \quad (8)$$

where ρ_d [M.L^{-3}] is the average deposit density, ρ_w [M.L^{-3}] is the fluid density, ρ_p [M.L^{-3}] is the SP specific density, N is the number of particles in a deposit site and a and b are constants, taken as equal to 1 and 1.3, respectively.

Figure 7 shows the porosity and permeability profiles measured in the porous medium for different flow velocities at the end of each injection. In Fig. 7b, K_0 and K are the initial and reduced permeability values, respectively. The permeability was obtained using Darcy's law, using the recorded pressure difference across the sample and the flow velocity.

The spatial distribution of the porosity, initially uniform, becomes slightly non-uniform after the SP

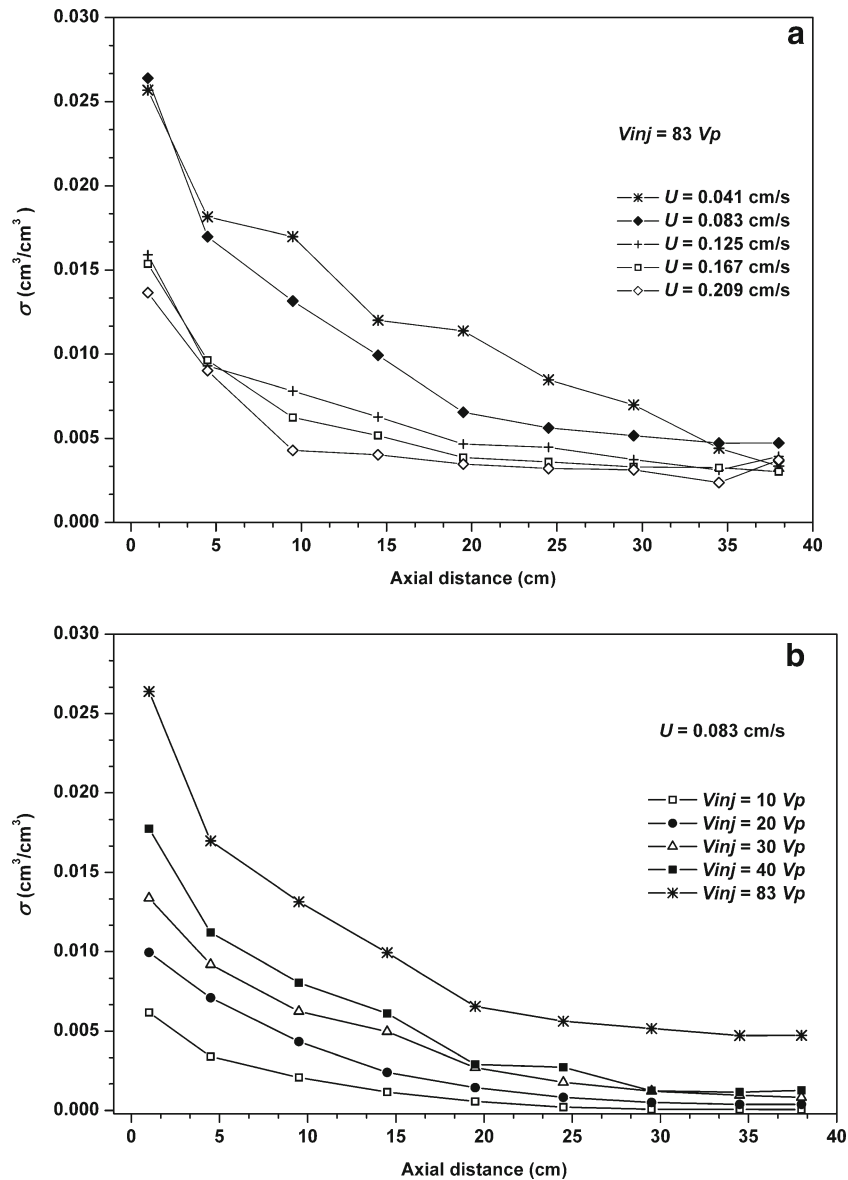


Fig. 5 Retention profile of the SP: **a** at the end of each injection for different flow velocities; and **b** in the porous medium at different experimental periods (number of pore volumes injected) for a single flow velocity ($U=0.083$ cm/s); parameters as defined in the text

injection (Fig. 7a). The porosity drops sharply at the entrance and then increases with depth. Thus, it is the first few centimetres of the porous medium that are most active in the deposition process, and which are usually the layer that becomes clogged. At a given depth, the drop in porosity is greater when the flow velocity is lower.

Permeability profiles (Fig. 7b) show clearly that the damage is not uniform in the porous space. Damage is important at the inlet to the porous medium, and decreases with depth. This non-uniform damage distribution increases when the flow velocity is low. For the lowest velocity ($U=0.041$ cm/s), the permeability in the first few centimetres of the porous medium is equal to 35 % of the initial permeability. Then, it increases with depth to reach the initial permeability in the last 10 cm of the porous medium. The damage to the porous medium is not only a function of the volume of the deposited particles, but is

also a function of the distribution of deposited particles in the porous space. Under conditions of low flow velocity, the suspended particles, especially the larger ones, are retained at the inlet (mainly by straining and sedimentation), resulting in severe and shallow damage to the porous medium. As the water velocity increases, the magnitudes of the drag and lift forces that act on SP near the surface of the grains will increase, and the volume where stagnant conditions apply (low velocity) is expected to decrease. Also, the increase in flow velocity may inhibit the straining of SP in small pore spaces. Higher flow velocities can carry the particles further, producing more gradual change in the deposition profile of the particles with depth. As a result, less important but deeper damage is observed. Therefore, the shape and magnitude of the porosity and the permeability profiles are sensitive to flow velocity.

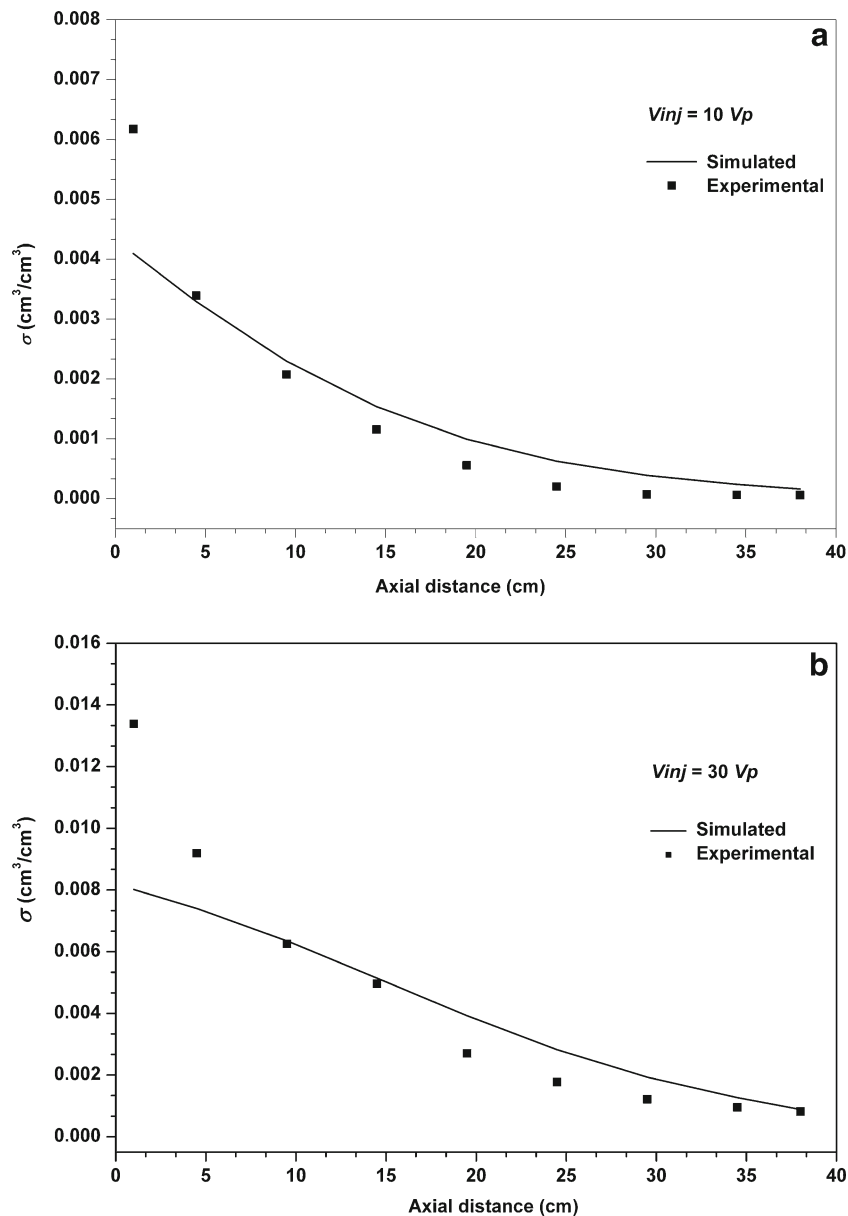


Fig. 6 Simulated retention profile of the SP along the length of the porous medium at different experimental periods: **a** $V_{inj}=10 V_p$; and **b** $V_{inj}=30 V_p$

Figure 8 shows the evolution of the overall permeability ratio (K_0/K) versus average retention ($\bar{\sigma}$) in the porous medium, for different tested velocities. The average retention ($\bar{\sigma}$) is defined as the ratio of the deposited SP volume V_{dp} to the total volume of the porous medium V_f . It is derived from the BTCs using the following equation (Bai and Tien 2000):

$$\bar{\sigma} = \frac{V_{dp}}{V_f} = \frac{1}{\rho_p L} \int_0^t U(C_0 - C) dt \quad (9)$$

Where ρ_p is the SP specific density ($\rho_p=2.6 \text{ g/cm}^3$), L is the length of the porous medium, and U is the Darcy velocity.

The average retention for all experiments does not exceed 3 % of the porous-medium volume, while permeability decreases by 1.7 orders of magnitude. This suggests that clogging does not depend primarily on the porosity reduction. Indeed, the deposition of particles leads to changes in tortuosity, surface area and pore structure of the porous medium.

Hydrodynamic effects are clearly visible at the beginning of the filtration process. In this stage of filtration, Fig. 8 reveals that experiments conducted with smaller flow velocities induced larger declines in permeability. This indicates that knowing the average retention is not sufficient to predict clogging by kaolinite, and clearly shows hydrodynamic effects. The observed differences in permeability reduction for a given average retention indicate the important role of deposition profile (Fig. 5a).

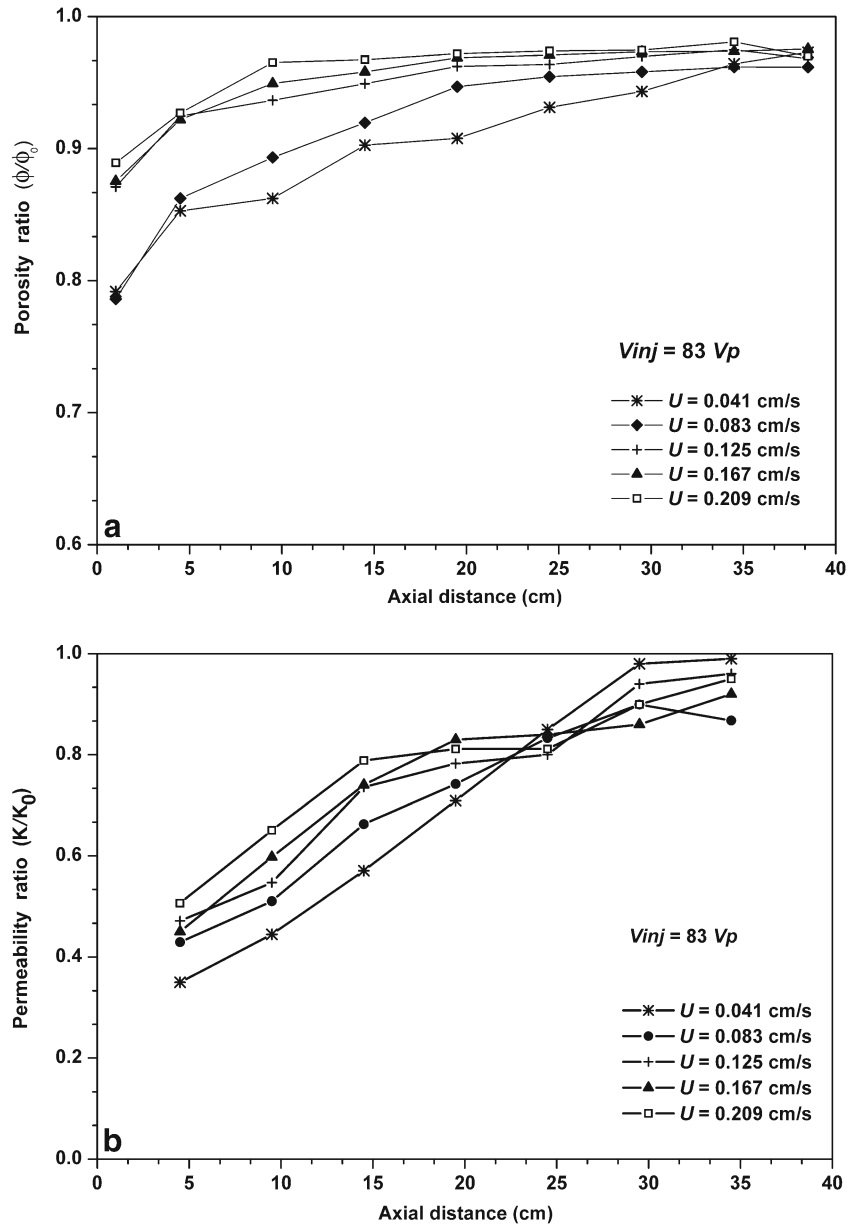


Fig. 7 Porosity (a) and permeability (b) profiles for different flow velocities as a function of the distance from the entrance of the porous medium

For long filtration times and when clogging is severe, the normalised permeability K_0/K increases proportionally with the average retention $\bar{\sigma}$. Thus, the permeability reduction due to deposition can be represented by the following empirical hyperbolic relationship:

$$\frac{K}{K_0} = \frac{1}{1 + \beta \bar{\sigma}} \quad (10)$$

with $\beta=21.74$ being the formation damage coefficient, which lumps together all the effects of retained particles on the permeability. These effects include changes in tortuosity, surface area, and pore structure of the porous medium.

Several other relationships have been suggested to relate the permeability reduction to particle retention (Herzig et al. 1970; Saripalli et al. 2000). The permeability reduction may be related to particle retention through the Kozeny-Carman equation as:

$$K = \frac{1}{C_s S^2 T^2} \frac{\phi^3}{(1 - \phi)^2} \quad (11)$$

where C_s is the shape factor ($C_s=2.5$ for granular media), S [L^{-1}] is the specific surface area based on the solid's volume, and T [L.L^{-1}] is the tortuosity.

When particles are deposited within a porous medium, they have the effect of increasing both the surface area and

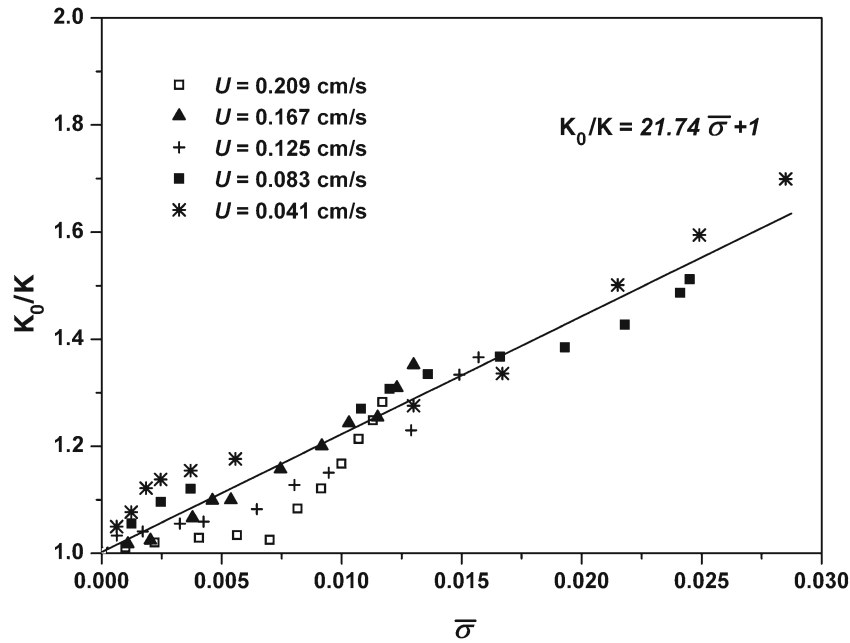


Fig. 8 Normalised permeability K_0/K evolution as a function of the average retention $\bar{\sigma}$ for different flow velocities

tortuosity, and reducing the porosity of the porous medium.

The change in porosity, as a consequence of the deposited particles, is evaluated from Eq. (7). The change in specific surface area is related to that of the clean porous medium and of the deposited particles by:

$$S = \frac{1}{1 - \phi} \left[(1 - \phi_0)S_0 + (1 - \phi_d) \frac{\sigma}{\rho_p} S_p \right] \quad (12)$$

Where ϕ_0 and S_0 are the porosity and the specific surface area of the clean bed, ϕ_d and S_p are the porosity and the specific surface area of the deposited particles, ϕ

and S are the porosity and the specific surface area of the dirty porous medium.

Tortuosity is related to porosity as follows (de Marsily 1986):

$$T = F\phi \quad (13)$$

where $F = \phi^{-m}$ is the formation factor (Archie 1942) given empirically as a function of porosity, with $m=1.3$ for a sandy medium.

Thus, the reduction in permeability is expressed as:

$$\frac{K}{K_0} = \frac{\phi^3}{\phi_0^3} \frac{(1 - \phi_0)^2}{(1 - \phi)^2} \frac{S_0^2}{S^2} \left(\frac{T_0}{T} \right)^2 \quad (14)$$

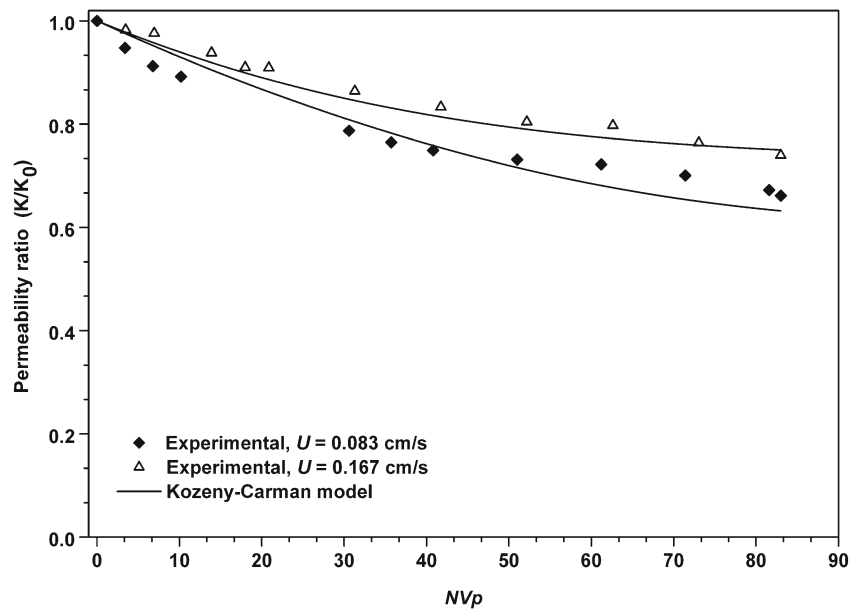


Fig. 9 Simulation of the global permeability decline using the Kozeny-Carman model

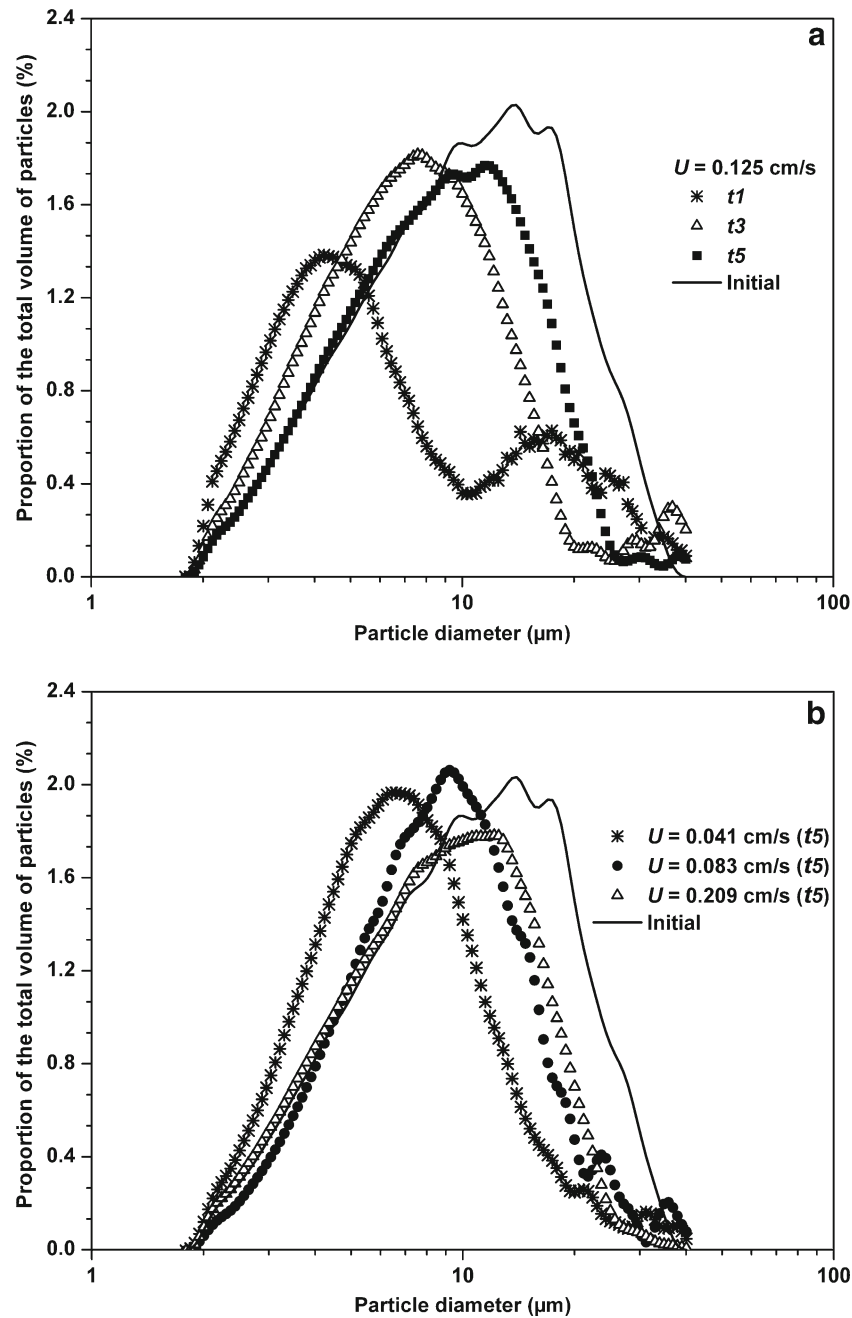


Fig. 10 Characterisation of the granulometric fractions of the SP travelling through the porous medium: **a** at different times during the experiment; and **b** after fixed volumes injected for different flow velocities. The initial injected SP spectrum is also shown, with a *solid line*

where K_0 [$L.T^{-1}$] and K [$L.T^{-1}$] are the initial and reduced permeability values, and T_0 is the initial tortuosity (clean bed).

The model (Eq. 14) is used to predict the global permeability decline in conjunction with the model derived during the present study (Eqs. 1–4). Figure 9 shows the results of the obtained simulation. The comparison shows good agreement between the modelling results and experimental data for the whole period of the experiments, suggesting that the model provides a satisfactory prediction of the global permeability decline resulting from deposition of solid particles in a porous medium.

Particle-size analysis of the recovered and deposited SP

This part of the paper presents an analysis of the particle-size distribution of the SP recovered at the column outlet and those deposited along the length of the porous medium. Effluent samples for particle-size analysis were taken periodically during the course of the experiment. Sampling times t_1 , t_2 , t_3 , t_4 and t_5 correspond to the number of pore volumes injected equal to 3, 15, 35, 58 and 83 V_p , respectively.

Figure 10a presents the granulometric spectra of the recovered SP from the experiment carried out with a

flow velocity of 0.125 cm/s. The initial injected SP spectrum is represented by a solid line. For clarity, only the spectra obtained at times t_1 , t_3 and t_5 are shown.

The results show that fine particles are the first to be transported to the outlet of the porous medium. Then, coarser particles appear gradually as the number of injected pore volumes increases. The size of SP in the effluent increased with increasing time. The modal diameter of the recovered SP increased from 5 to 12 μm when the number of pore volumes injected increased from 3 to 83 V_p . The same behaviour was observed by Bradford et al. (2006). At the beginning of the filtration process, the coarser particles were preferentially subject to removal early in the porous medium. This behaviour is mainly due to the fact that the coarser particles are most susceptible to trapping and sedimentation effects. Gradually, due to the accumulation of deposited particles, the pore velocities and pressures increase sufficiently to induce the transport of coarser particles deeper into the column, towards the porous-medium outlet. The granulometric spectrum of the recovered particles approaches the particle-size distribution initially injected, as the injected volume increases.

The impact of flow velocity on the particle-size distribution of the SP that reach the outlet of the porous medium is clearly demonstrated in Fig. 10b, which presents the SP granulometric size distribution of samples collected at time t_5 (83 V_p) for three different flow velocities. The modal diameter of the recovered particles increases with flow velocity. At low flow velocity, the recovered particles are mainly the smaller ones, because the hydrodynamic forces exerted by the flow on the particles are insufficient to mobilise larger particles, which remain trapped.

However, independent of the flow velocity, coarse particles larger than around 24 μm were practically all retained in the porous medium. The ratios of these particle sizes to the mean grain size exceed 0.06. These ratios are greater than the 0.05 reported by Herzig et al. (1970), and significantly greater than the 0.005 reported by Bradford et al. (2003). This indicates that straining plays a dominant role in the removal of these particles, without neglecting their deposition by sedimentation.

To study the influence of the number of pore volumes injected (NV_p) on the particle-size distribution of the deposited particles at different depths, identical tests were undertaken (for $U=0.083$ cm/s), with the test being stopped at different values of NV_p . The particle-size spectra of the SP deposited in the porous medium were determined. The modal particle diameters as a function of the axial distance from the entrance to the porous medium are shown in Fig. 11. At the beginning of the filtration process ($V_{inj}=3$ V_p), the coarser particles (modal diameter around 16 μm) are mainly deposited at the entrance of the porous medium, and a strong decrease in the modal diameter with depth is observed (to around 5 μm at the outlet). As the injected volume increases, the accumulation of deposited particles induces an increase in pore velocities and pressures, which allows more coarse particles to penetrate more deeply into the porous medium. Also, as discussed by Roque et al. (1995), the probability of re-entrainment strongly increases with the particle size and flow rate. Thus, the modal diameter of the deposited particles, at a given depth, increases and approaches the modal diameter of the SP initially injected (shown on Fig. 11 by a dotted line). This evolution correlates with the granulometric spectra of the SP collected in the effluent (Fig. 10a), which

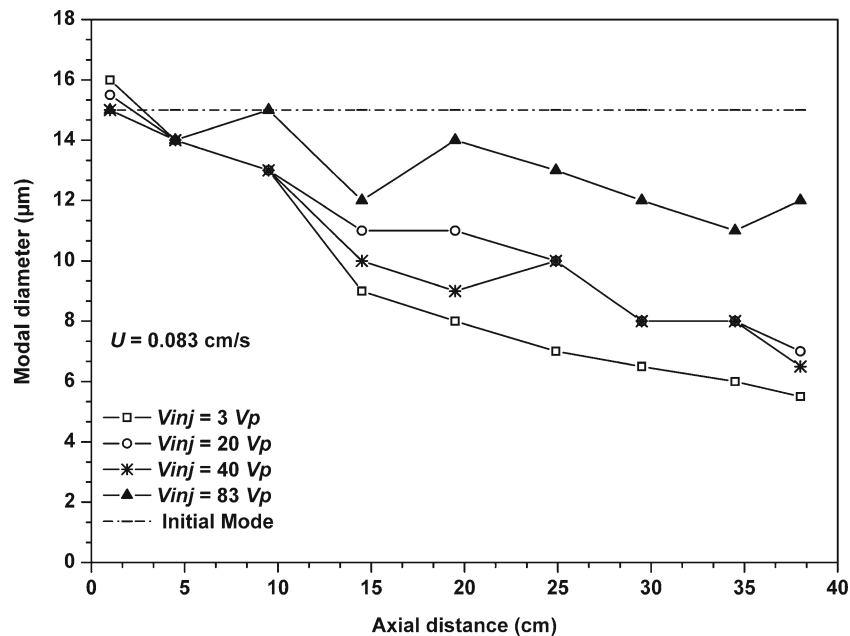


Fig. 11 Granulometric analysis of the deposited SP at different NV_p injected versus the porous medium depth

shows an increase in the size of SP recovered with increasing time.

Conclusions

Physical clogging processes in a saturated porous medium were investigated by performing step-input injections of polydisperse suspended particles. Long-term tracer tests were carried out at various flow velocities. The influences of flow velocity, duration of filtration, and particle polydispersity on the hydraulic characteristics of the porous medium were examined.

It was found that low flow velocity promotes the deposition of suspended particles, especially the larger ones, near the entrance to the porous medium, resulting in severe and shallow damage. High flow velocities carry the particles deeper into the porous medium, producing more gradual changes in the deposition profile with depth. As a result, less important but deeper damage was observed. The damage is not only a function of the volume of deposited particles but is also a function of the deposition profile of the retained particles in the porous space.

Particle-size analyses indicate that the particle-size distribution of the recovered particles changed with time, while that of the deposited particles changed with depth and time. At the beginning of the filtration process, larger particles were mainly retained at the entrance of the medium by the mechanism of straining. A decrease in the modal diameter of the deposited particles with depth was observed. Fine particles are the first to be transported to the outlet of the porous medium. As the injection volume increases, due to the accumulation of deposited particles, the pore velocities and pressures increase sufficiently to cause the transport of large particles more deeply into the porous medium, and gradually the size of the particles in the effluent increases. Particle-size distribution of the effluent and how this changes with time are highly dependent on flow velocity (the particle size increases with flow velocity). Changes in particle-size distribution with time occur more rapidly when the flow velocity is high.

From the results and analysis performed in this study, it appears that straining is one of the dominant mechanisms in the filtration of polydisperse micro-size particles (>2 μm).

Acknowledgements The authors would like to thank the Associate Editor and the anonymous reviewers for their valuable comments and constructive criticism to improve the manuscript.

References

- Ahfir N-D, Wang HQ, Benamar A, Alem A, Massei N, Dupont J-P (2007) Transport and deposition of suspended particles in saturated porous media: hydrodynamic effect. *Hydrogeol J* 15:659–668
- Ahfir N-D, Benamar A, Alem A, Wang HQ (2009) Influence of internal structure and medium length on transport and deposition of suspended particles: a laboratory study. *Transp Porous Med* 76:289–307
- Archie GE (1942) The electrical resistivity log as an aid in determining some reservoir characteristics. *Trans AIME* 146:54–67
- Bai R, Tien C (2000) Effect of deposition in deep-bed filtration: determination and search of rate parameters. *J Colloid Interface Sci* 231:299–311
- Boller MA, Kavanaugh MC (1995) Particle characteristics and headloss increase in granular media filtration. *Water Res* 29:1139–1149
- Bouwer H (2002) Artificial recharge of groundwater: hydrogeology and engineering. *Hydrogeol J* 10:121–142
- Bradford SA, Yates SR, Bettahar M, Simunek J (2002) Physical factors affecting the transport and fate of colloids in saturated porous media. *Water Resour Res*. doi:10.1029/2002WR001340
- Bradford SA, Simunek J, Bettahar M, Van Genuchten MT, Yates SR (2003) Modeling colloid attachment, straining, and exclusion in saturated porous media. *Environ Sci Technol* 37:2242–2250
- Bradford SA, Tadassa YF, Pachepsky Y (2006) Transport of Giardia and manure suspensions in saturated porous media. *J Environ Qual* 35:749–757
- Brovelli A, Malaguerra F, Barry DA (2009) Bioclogging in porous media: model development and sensitivity to initial conditions. *Environ Model Softw* 24:611–626
- Brown DG, Stencel JR, Jaffé PR (2002) Effect of porous media preparation on bacteria transport through laboratory columns. *Water Res* 36:105–114
- Compere F, Porel G, Delay F (2001) Transport and retention of clay particles in saturated porous media: influence of ionic strength and pore velocity. *J Contam Hydrol* 49:1–21
- de Marsily G (1986) Quantitative hydrogeology: groundwater hydrology for engineers. Academic, New York
- Detay M (1993) Le forage d'eau: Réalisation, entretien, réhabilitation [Water drilling: realisation, maintenance, rehabilitation]. Masson, Paris
- Hand VL, Lloyd JR, Vaughan DJ, Wilkins MJ, Boulton S (2008) Experimental studies of the influence of grain size, oxygen availability and organic carbon availability on bioclogging in porous media. *Environ Sci Technol* 42:1485–1491
- Herzig JP, Leclerc DM, Le Goff P (1970) Flow of suspension through porous media: application to deep bed filtration. *Indian Eng Chem* 62:8–35
- Jegatheesan V, Vigneswaram S (2000) Transient stage deposition of submicron particles in deep bed filtration under unfavourable conditions. *Water Res* 34:2119–2131
- Johnson WP, Xiqing L, Shoeleh A (2007) Deposition and re-entrainment dynamics of microbes and non-biological colloids during non-perturbed transport in porous media in the presence of an energy barrier to deposition. *Adv Water Resour* 30:1432–1454
- Kehat E, Lin A, Kaplan A (1967) Clogging of filter media. *Ind Eng Chem Process Des Dev* 6:48–55
- Khilar KC, Fogler HS (1984) The existence of a critical salt concentration for particle release. *J Colloid Interface Sci* 101:214–224
- Lee J, Koplik J (2001) Network model for deep bed filtration. *Phys Fluids* 13:1076–1086
- Mays DC, Hunt JR (2005) Hydrodynamic aspects of particle clogging in porous media. *Environ Sci Technol* 39:577–584
- Mays DC, Hunt JR (2007) Hydrodynamic and chemical factors in clogging by montmorillonite in porous media. *Environ Sci Technol* 41:5666–5671
- McGechan MB, Lewis DR (2002) Transport of particulate and colloid-sorbed contaminants through soil, part 1: general principles. *Biosyst Eng* 83:255–273
- Moghadasli J, Müller-Steinhagen H, Jamialahmadi M, Sharif A (2004) Theoretical and experimental study of particle movement and deposition in porous media during water injection. *J Petrol Sci Eng* 43:163–181

- Ochi J, Vernoux J-F (1999) A two-dimensional network model to simulate permeability decrease under hydrodynamic effect of particle release and capture. *Transp Porous Med* 37:303–325
- Reddi LN, Xiao M, Malay GH, Lee IM (2005) Physical clogging of soil filters under constant flow rate versus constant head. *Can Geotech J* 42:804–811
- Roque C, Chauveteau G, Renard M, Thibault G, Bouteau M (1995) Mechanisms of formation damage by retention of particles suspended in injected water. *Eur Formation Damage Conference*, The Hague, SPE paper 30110, SPE, Tulsa, OK
- Saripalli KP, Sharma MM, Bryant SL (2000) Modeling injection well performance during deep-well injection of liquid wastes. *J Hydrol* 227:41–55
- Sen TK, Khilar KC (2006) Review on subsurface colloids and colloid-associated contaminant transport in saturated porous media. *Adv Colloid Interface Sci* 119:71–96
- Shellenberger K, Logan BE (2002) Effect of molecular scale roughness of glass beads on colloidal and bacterial deposition. *Environ Sci Technol* 36:184–189
- Tong M, Johnson WP (2006) Excess colloid retention in porous media as a function of colloid size, fluid velocity, and grain angularity. *Environ Sci Technol* 40:7725–7731
- Torkzaban S, Bradford SA, Walker SL (2007) Resolving the coupled effects of hydrodynamics and DLVO forces on colloid attachment in porous media. *Langmuir* 23:9652–9660
- Veerapaneni S, Wiesner MR (1997) Deposit morphology and head loss development in porous media. *Environ Sci Technol* 31:2738–2744
- Vigneswaran S, Suazo Ronillo B (1987) A detailed investigation of physical and biological clogging during artificial recharge. *Water Air Soil Pollut* 35:119–140
- Wegelin M (1996) *Surface water treatment by roughing filters: a design, construction and operation manual*. Swiss Federal Institute for Environmental Science and technology (EAWAG) and Department Water and Sanitation in Developing Countries (SANDEC), Dübendorf, Switzerland
- Xu SP, Saiers JE (2009) Colloid straining within water-saturated porous media: effect of colloid size nonuniformity. *Water Resour Res.* doi:10.1029/2008WR007258
- Zamani A, Maini B (2009) Flow of dispersed particles through porous media: deep bed filtration. *J Petrol Sci Eng* 69:71–88
- Zhang S, Tan RBH, Neoh KG, Tien C (2000) Electrofiltration of aqueous suspension. *J Colloid Interface Sci* 228:393–404